GEOPHYSICAL RESEARCH LETTERS, VOL. 17, NO. 10, PAGES 1649-1652, SEPTEMBER 1990

LOW-FREQUENCY RADIO EMISSIONS AT NEPTUNE

W. S. Kurth,[1] D. D. Barbosa,[2] D. A. Gurnett,[1] R. L. Poynter,[3] and I. H. Cairns[1]

[1]Department of Physics and Astronomy, The University of Iowa
[2]Institute of Geophysics and Planetary Physics, University of California, Los Angeles
[3]Jet Propulsion Laboratory

Abstract. The Voyager 2 plasma wave receiver detected weak radio emissions from Neptune's magnetosphere in the frequency range of 3 - 60 kHz. The emissions occurred in bursts lasting for typically 1.5 hours, often occurring twice per planetary rotation. Most of these radio bursts were detected within several degrees of the magnetic equatorial plane. During the passage through the magnetosphere, electrostatic upper hybrid resonance bands were observed close to the magnetic equator in conjunction with intensifications of the radio emissions at frequencies close to and above the upper hybrid bands. Further, near closest approach, the radio emissions were observed to cross the right-hand cutoff frequency with no apparent attenuation. We conclude that the Neptunian radio emissions below about 60 kHz are produced by mode conversion from the upper hybrid waves and propagate in the ordinary mode into beams within about 12° of the magnetic equator. There is also evidence of an extraordinary mode emission at about 60 kHz which is apparently generated by an entirely different source from the escaping continuum radiation.

Introduction

Neptune, like Jupiter, Saturn, and Uranus, exhibits a rich radio spectrum which, in the case of Neptune, extends to approximately 1 MHz [Warwick et al., 1989; Gurnett et al., 1989]. The plasma wave receiver observed weak, diffuse radio emissions down to about 3 kHz. Generally, the radio emissions at Neptune are weak, relative to Jupiter and Saturn, but comparable to those of Uranus.

At Neptune, a strong case can be made for identifying the low frequency (3 - 60 kHz) radio component as escaping nonthermal continuum radiation [Kurth et al., 1981], that is, ordinary mode radio emissions generated via mode conversion from upper hybrid bands located at the magnetic equator. Herein we describe the observations which lead to this conclusion. The observations were made by the Voyager 2 plasma wave receiver during an interval lasting for about 10 days around the closest approach to Neptune. Limited evidence for extraordinary mode emissions at about 60 kHz from an apparently different source is also given. For a description of the Voyager 2 plasma wave instrument see Scarf and Gurnett [1977].

Spectral and Temporal Character of the Low Frequency Radio Emissions

The plasma wave receiver began detecting radio emissions in the 31-kHz channel during August 21, 1989 (day 233) some four days prior to closest approach and 200 R_N (Neptune radius = 24,762 km) sunward of the planet. Bursts of emissions in the frequency range of about 3 kHz to 60 kHz were observed through closest approach and as late as September 2, (day 245), some 450 R_N beyond the planet. On the inbound trajectory the bursts were observed most commonly in the 31.1-kHz channel whereas during the outbound trajectory, the bursts were most common at 17.8 kHz. Often, the bursts appeared with durations of about one and one-half hours with as many as two bursts occurring per planetary rotation period which has been determined to be 16.11 hr by Warwick et al. [1989].

The radio emissions were so weak that they were only marginally detectable except during the day of closest approach; the Voyager plasma wave spectrum analyzer suffers from an effective decrease in sensitivity as a result of a failure in the Flight Data System onboard the spacecraft. Figures 1 and 2 illustrate the nature of the radio emissions observed on the inbound and outbound legs of the trajectory, respectively. In these figures, the intensity of waves are plotted as a function of frequency (ordinate) and time (abscissa) with the intensity scaled according to the scale at the right. The data used in compiling Figures 1 and 2 are from the 16-channel spectrum analyzer. The white line in the figures is the electron cyclotron frequency f_{ce}[Hz]= 28|B|[nT] where |B| is based on the OTD2 magnetic field model outside of about 3 R_N and the measured |B| inside thereof [N. F. Ness, personal communication, 1990]. The very intense noise events centered at about 0253 and 0516 SCET are caused by dust impacts on the spacecraft [Gurnett et al., 1989].

The radio emissions in Figure 1 are seen generally above about 3 kHz and begin to intensify and spread in frequency at about 2300 spacecraft event time (SCET) on August 24. The maximum frequency of the emission is sometimes observed to be near 20 - 30 kHz as seen early in Figure 1. As the spacecraft approaches the planet, the emission spreads to the highest frequency channel (56.2 kHz) and presumably into the range of the planetary radio astronomy receiver [Warwick et al., 1989]. The maximum intensity and the minimum low frequency cutoff occur shortly after the beginning of August 25, nearly coincident with the brief burst of noise between 300 Hz and 3 kHz at about 0023 SCET. This noise burst occurs on the magnetic equator and corresponds to electron Bernstein emissions [Barbosa et al., 1990], the upper band of which, the upper hybrid resonance band, is thought to be the source of the radio emissions as will be discussed below. Figure 1 shows the smoothly varying temporal nature of the radio emission as well as the lack of spectral features. The radio emission appears to intensify in the 56.2-kHz channel at around 0300 SCET, but we will argue below that this signal is from an entirely different radio source. Figure 2 shows the occurrence of the emissions on the outbound leg of the trajectory. As on the inbound leg, the emissions show a broad peak in intensity and expand to the lowest frequency at about the same time as the occurrence of Bernstein mode emissions at about 0759

Paper number 90GL01263
0094-8276/90/90GL-01263$03.00

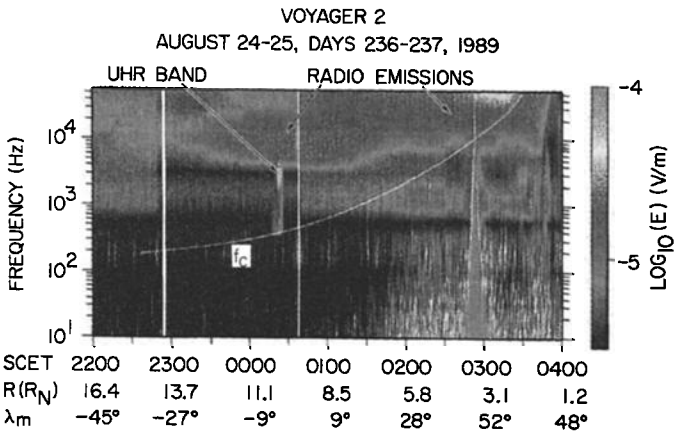

Fig. 1. A frequency-time spectrogram constructed from the Voyager 2 plasma wave 16-channel spectrum analyzer data showing the variation of amplitude and bandwidth of Neptune's low-frequency radio emissions.

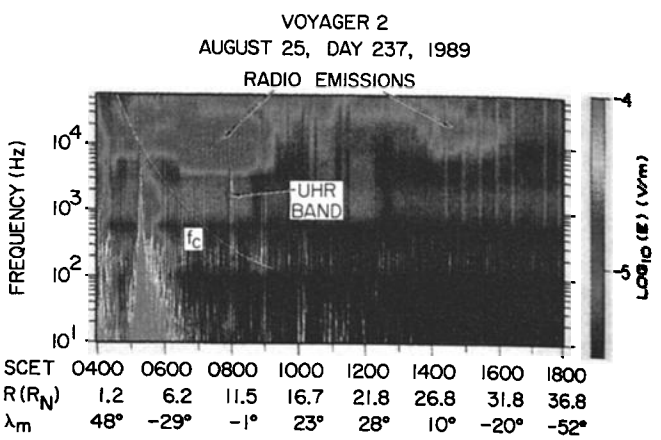

Fig. 2. A display similar to Figure 1 of the outbound plasma wave spectrum showing similar aspects of the low-frequency radio emissions.

SCET, again at the magnetic equator. Figure 1 shows that the radio emissions intensify and spread in frequency a second time, centered around 1445 SCET, near another magnetic equator crossing.

Figure 3 provides a better idea of the form of the spectrum based on the wideband waveform measurements which were available occasionally throughout the encounter. These measurements are highly superior to the spectrum analyzer data in terms of the spectral resolution and are not subject to degradation by the Flight Data System failure. Three sample spectra are shown from different locations to show the range of spectral variability of the radio emission. Based on analyses of high temporal resolution frequency-time spectrograms, it is clear that the radio emission spectrum does not show drastic changes on time scales of a minute or less. The spectra show the presence of narrowband components superimposed on the continuum background. This characteristic is reminiscent of nonthermal continuum radiation observed at Earth [Kurth et al., 1981] and at Jupiter [Gurnett et al., 1983]. In the upper and lower spectra in Figure 3, there appears to be a broad minimum centered about 7.2 kHz. This coincides with the frequency of a notch filter in the receiver designed to filter out the third harmonic of the spacecraft power supply, so it is unlikely that there are really two distinct bands comprising the spectrum.

The power fluxes in the spectra shown in Figure 3 do not exceed 10^{-15} W/m^{2}Hz. Unfortunately, wideband data are not available closer to the peaks in the radio emission intensity, hence, we do not have an accurate measurement of the maximum radio emission power flux. Using Figures 1 and 2 as a guide, however, it is apparent that the peak is not much more than a factor of 3 greater than at these times in units of electric field intensity, or a factor of 10 greater in power flux. Hence, the peak power flux for these emissions is probably about 10^{-14} W/m^{2}Hz.

It is important to note that the low frequency radio emissions are well above the electron plasma frequency in the solar wind; Langmuir waves upstream of the bow shock were at a frequency of about 562 Hz [Gurnett et al., 1989]. We conclude that these radio emissions are not trapped within the magnetospheric cavity as is the case with the lower frequency components of nonthermal continuum radiation at Earth [Gurnett, 1975], Jupiter [Scarf et al., 1979], Saturn [Kurth et al., 1982], and Uranus [Kurth et al., 1990].

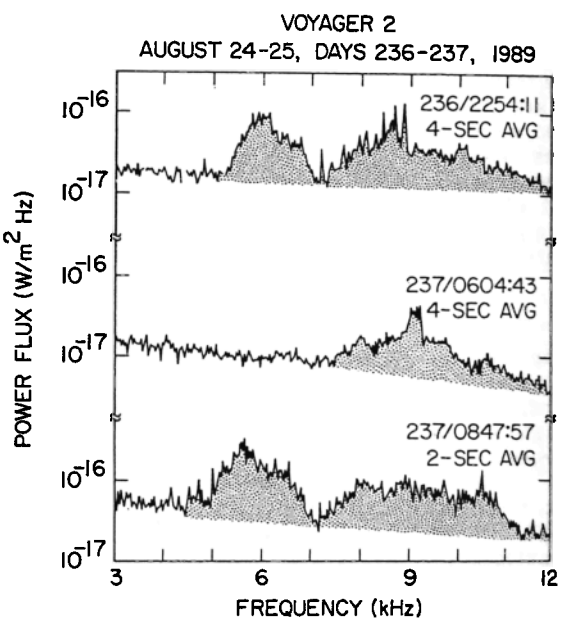

Fig. 3. Three sample detailed spectra of the escaping continuum radiation showing the characteristic narrowband components superimposed on a relatively smooth continuum.

Identification of the Propagation Mode

The spectrogram in Figure 1 provides an excellent indication of the mode of propagation of the low frequency radio emissions. Radio emissions propagate in either the ordinary mode or the extraordinary mode. Each of these modes cuts off at a specific frequency, determined by the magnetic field strength and the plasma density. Both before and after closest approach the radio emission apparently cuts off at the local electron plasma frequency. This is especially apparent at the two magnetic equator crossings at 0023 and 0759 SCET where the radio emission extends down to the upper hybrid resonance band which, for these conditions, is nearly equal to the electron plasma frequency. Ordinary-mode emissions cut off at the local electron plasma frequency. Another observation which is crucial to the mode identification can be found in Figure 1. From about 0245 to 0325 SCET the radio emission

between about 10 and 40 kHz can be seen to cross through the f_{ce} profile superimposed on the spectrogram without any significant change in amplitude. The extraordinary-mode cutoff occurs just above the cyclotron frequency when $f_{pe} < f_{ce}$, where $f_{pe}[Hz] = 8980 n_e^{1/2}$ and n_e is the electron density in units of cm^{-3}. Hence, the lack of a cutoff near f_{ce} is also consistent with the ordinary mode identification. The emission does, however, exhibit an abrupt cutoff shortly after crossing the cyclotron frequency between about 0345 and 0350 SCET, and we could interpret this as the cutoff at the plasma frequency. This cutoff indicates the plasma frequency is rising rapidly at about 0345 SCET, consistent with the high ionospheric densities reported by the radio science team [Tyler et al., 1989] and the extremely close approach (~0.18 R_N above the cloud-tops). At 0350 SCET the cutoff is at 56 kHz, corresponding to a density of 39 cm^{-3}. Since the cutoff shows no evidence of decreasing its rate of ascent within the plasma wave receiver's spectral range, the respective plasma density could be much greater. An alternative interpretation of the rapidly-rising 'cutoff' between 0345 and 0350 SCET is that the radio waves are shadowed by a high-density region remote from the spacecraft. In this interpretation the observed 'cutoff' is an upper limit to f_p. A third interpretation of the cutoff is that it is the L=0 cutoff [Stix, 1962] of Z-mode waves, which would imply the plasma frequency is even higher.

The more intense emission above 40 kHz exhibits a clear cutoff just above f_{ce} at 0325 SCET as well as at f_p near 0350. Therefore, the 60-kHz emission must be primarily extraordinary mode radiation with a lower level of ordinary mode emissions which are probably the high-frequency extension of the lower-frequency component. This X-mode radiation has a different source than the lower frequency emission.

It is interesting to look at the effects around the extraordinary-mode cutoff on the outbound leg in Figure 2 between about 0425 and 0500 SCET. In this example, the radio emission above f_{ce} but below about 40 kHz is again not observed to cut off as it crosses the extraordinary-mode cutoff just above f_{ce}, but the intensity of emissions below the f_{ce} profile is actually greater than those above the cutoff. We interpret the emissions below f_{ce} on the outbound leg as being a combination of the ordinary mode radio emissions plus Z-mode radiation which is confined to propagate between the L=0 and R=0 cutoffs [Stix, 1962]. This interpretation requires that f_p at this time be less than f_{ce}. There is other evidence in the plasma wave spectrum and the plasma observations [Belcher et al., 1989] which indicates that $f_{pe} < f_{ce}$ prior to about 0500 SCET.

Beam Width and Direction

Figure 4 shows a series of radio emissions observed on the outbound leg of the encounter at distances ranging from 170 to 290 R_N. Each event is plotted on a common time scale and aligned such that the magnetic equator crossings, as indicated by the vertical dashed line, are coincident. At the bottom, a typical profile of magnetic latitude of the spacecraft as a function of time is indicated, depending on whether the spacecraft is northbound (S → N) or southbound (N → S). As can be seen, there is some variation in position about the equatorial plane. Nevertheless, the illustration shows that the emissions have only a limited extent in magnetic latitude and that they are emitted in the general direction of several degrees from the magnetic equator. The exception to this is the emission observed near closest approach and at high magnetic latitudes. Gurnett et al. [1989] showed that the more distant detections of the low frequency radio emissions occurred twice per planetary rotation, specifically near the magnetic equatorial plane. An average beamwidth of all clearly definable events at 17.8 and 31.1 kHz and at distances of greater than about 35 R_N gives a full width of about 23° and a standard deviation of some 11°. As can be seen in Figure 4, these events only exceed the noise threshold of the instrument by about 2 db, so it is not possible to formally calculate a full width at half maximum and account for the expected $1/R^2$ dependence of the amplitude. This type of analysis is further hampered by the effects of the Flight Data System failure.

In spite of the shortcomings of the beam-width determination, the value is sufficient to compare to existing theory on the beaming of radio emissions generated via mode conversion from upper hybrid resonance emissions [Jones, 1976]. The theory predicts beaming at an angle α with respect to the magnetic equator of $\alpha = \tan^{-1}(f_{ce}/f_{pe})^{1/2}$ measured at the conversion position where the frequency of the wave is equal to f_{pe}. The upper hybrid events shown in Figures 1 and 2 provide an estimate for f_{pe} and f_{ce} for waves emitted at $f_{UH} = (f_{ce}/f_{pe})^{1/2} = 3.1$ and 1.8 kHz, respectively. The theoretical beaming angles for these two instances are 20° and 21°, respectively. The theory would suggest both a northern and southern beam. Although there is some evidence of a bifurcation (a relative minimum in the middle of the event) in the burst profile in a couple of the events depicted in Figure 4, a source of finite spatial extent would tend to smear the two beams out and we should compare twice the theoretical beaming angle to the measured full width of the events.

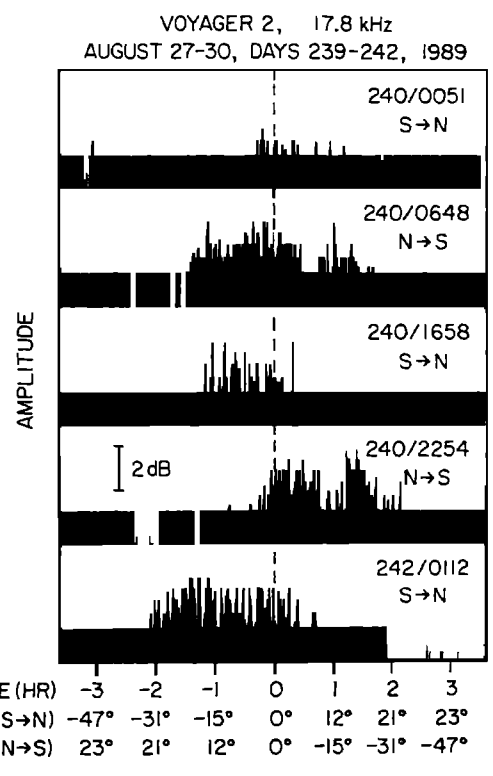

Fig. 4. A selection of radio emission events observed at 17.8 kHz on the outbound trajectory demonstrating the relationship of the emissions with the magnetic equator and their latitudinal extent.

Analysis of the width in magnetic latitude of the lowest frequency extent of the radio emission in Figure 1 shows a measure of consistency with the beaming theory. The emission spreads down to a few kHz over the period from about 2330 SCET on August 24 to around 0130 SCET on the following day. During this interval the spacecraft traversed from about -18° to about 18° in magnetic latitude, consistent with a theoretical beaming angle of about 20°. Of course, we have measured the beam width primarily at 17.8 kHz (although some events at 31.1 kHz were included in the average) so we must be wary of a systematic change in beam width with increasing frequency. Unfortunately, we do not have in situ measurements of either f_{pe} or f_{ce} at the magnetic equator between about 1.7 and 10 R_N, the region within which the 17.8- and 31.1-kHz emissions must be generated. Inverting the problem, though, and using the observed beam width of about 23° as twice the beaming angle α, we can estimate the ratio f_{ce}/f_{pe} required to give a beaming angle of 11.5°. The result is $f_{pe}/f_{ce} \simeq 24$ at the source of the 17.8- and 31.1-kHz emissions. This suggests that substantial plasma densities ($3 < n_e < 10$ cm^{-3}) occur in the magnetic equatorial plane inside of 10 R_N. Such a conclusion might suggest the equatorial plasma density at 1.7 R_N is significantly greater than the value of ~ 1 cm^{-3} reported by Belcher et al. [1989] at 0420 SCET.

Source of the Radio Emissions

It was demonstrated in Figures 1 and 2 that the radio emission intensity maximized and the emissions spread to the lowest frequencies near crossings of the magnetic equatorial plane. Figures 1 and 2 also strongly suggested a connection between the radio waves and the upper band in the Bernstein mode emissions. This upper band is commonly referred to as the upper hybrid resonance band since it generally corresponds to the cyclotron harmonic band coinciding with f_{UH}. It is generally accepted that the upper hybrid bands are the source of weak radio emissions in other planetary magnetospheres. Given that the electrostatic emissions were obvious at both magnetic equatorial crossings, we suggest that the upper hybrid band exists for a broad range of radial distances and, since the density in the plasma sheet likely increases with decreasing distance to Neptune, probably covers the frequency range from about 3 kHz to about 30 - 60 kHz closer to the planet; the upper frequency limit suggests the maximum upper hybrid frequency in the source region. At each radial distance, a slightly different frequency radio emission is produced, giving rise to the broadband radio emission spectrum observed. The existence of the narrowband components (Figure 3) occasionally seen superimposed on the spectrum is consistent with narrowband upper hybrid bands as a source. Most conclusive, however, is that the theory for mode conversion from upper hybrid waves to electromagnetic radio emissions is most efficient for the ordinary mode [Budden and Jones, 1987], consistent with the polarization measurement afforded by the cutoff analysis provided above.

We conclude that the Neptunian radio emissions below about 60 kHz are analogous to escaping continuum radiation at the Earth and are produced by mode conversion from the electrostatic upper hybrid waves and propagate in the ordinary mode into beams within about 12-20° of the magnetic equator. Similar radio emissions have been observed at the Earth and all the outer planets. We have also shown evidence of extraordinary mode emissions just before closest approach at about 60 kHz which, because of their polarization, are likely a different type of radio emission from the escaping continuum. We have not identified a source for the extraordinary mode emissions.

Acknowledgements. We greatfully acknowledge N. F. Ness and the Voyager magnetometer team for the provision of the OTD2 magnetic field model and the measured magnetic field. The research at the University of Iowa was supported by the National Aeronautics and Space Administration through Contract 957723 with the Jet Propulsion Laboratory.

References

Barbosa, D. D., W. S. Kurth, I. H. Cairns, D. A. Gurnett, and R. L. Poynter, Electrostatic electron and ion cyclotron harmonic waves in Neptune's magnetosphere, Geophys. Res. Lett., this issue, 1990.

Belcher, J. W. et al., Plasma observations near Neptune: Initial results from Voyager 2, Science, 246, 1478, 1989.

Budden, K. G., and D. Jones, Conversion of electrostatic upper hybrid emissions to electromagnetic O and X mode waves in the Earth's magnetosphere, Ann. Geophys., 5A, 21, 1987.

Gurnett, D. A., The Earth as a radio source: The non-thermal continuum, J. Geophys. Res., 80, 2751, 1975.

Gurnett, D. A., W. S. Kurth, and F. L. Scarf, Narrowband electromagnetic emissions from Jupiter's magnetosphere, Nature, 302, 385, 1983.

Gurnett, D. A. et al., First plasma wave observations at Neptune, Science, 246, 1494, 1989.

Jones, D., Source of terrestrial non-thermal radiation, Nature, 260, 686, 1976.

Kurth, W. S., D. A. Gurnett, and R. R. Anderson, Escaping non-thermal continuum radiation, J. Geophys. Res., 86, 5519, 1981.

Kurth, W. S., F. L. Scarf, J. D. Sullivan, and D. A. Gurnett, Detection of non-thermal continuum radiation in Saturn's magnetosphere, Geophys. Res. Lett., 9, 889, 1982.

Kurth, W. S., D. A. Gurnett, and M. D. Desch, Continuum radiation at Uranus, J. Geophys. Res., 95, 1183, 1990.

Scarf, F. L. and D. A. Gurnett, A plasma wave investigation for Voyager, Space Sci. Rev., 21, 289, 1977.

Scarf, F. L., D. A. Gurnett, and W. S. Kurth, Jupiter plasma wave observations: An initial Voyager 1 overview, Science, 204, 991, 1979.

Stix, T. H., The Theory of Plasma Waves, McGraw-Hill, New York, 1962.

Tyler et al., Voyager radio science observations of Neptune and Triton, Science, 246, 1466, 1989.

Warwick, J. W. et al., Voyager planetary radio astronomy at Neptune, Science, 246, 1498, 1989.

W. S. Kurth, D. A. Gurnett, I. H. Cairns, Department of Physics and Astronomy, The University of Iowa, Iowa City, Iowa 52242

D. D. Barbosa, Institute of Geophysics and Planetary Physics, University of California, Los Angeles, California 90024

R. L. Poynter, Jet Propulsion Laboratory, 4800 Oak Grove Drive, Pasadena, California 91109

(Received April 12, 1990;
Accepted April 30, 1990.)